Proceedings of ASME Turbo Expo 2011
GT2011
June 6-10, 2011, Vancouver, British Columbia, Canada

GT2011-45304

COMPRESSIBLE AND INCOMPRESSIBLE LARGE EDDY SIMULATION OF A PREMIXED DUMP COMBUSTOR

Terence Ma*
Andreas M. Kempf
Department of Mechanical Engineering
Imperial College London
SW7 2AZ
United Kingdom
Email: terence.ma03@imperial.ac.uk
a.kempf@imperial.ac.uk

ABSTRACT

Premixed combustion in the ORACLES dump combustor is investigated by Large-Eddy Simulation. The results are compared with experimental measurements of mean and fluctuating velocities at various points inside the combustor. The LES is performed with the in-house PsiPhi code, which has been modified to account for compressibility so that flame-acoustic interactions can be studied. The modifications include the use of proper boundary conditions that are based on the Navier-Stokes Characteristic Boundary Conditions (NSCBC) [1]. A fixed velocity and temperature inlet as well as a partially reflecting outlet are selected. The reaction rate is modelled using algebraic expressions for the generalised flame surface density (FSD) Σ_{gen}. A selection of FSD models [2] were previously tested using the incompressible version of PsiPhi and this work examines three additional models. Previous incompressible works [2, 3] on this setup emulated the effect of acoustic oscillations by introducing sinusoidal pulsations at the inlet with a frequency of 50Hz. We apply the same technique for the simulations and match the results with those from the modified compressible version, albeit for a compact domain which cannot be expected to capture the lowest acoustic frequencies. Apart from assessing performance, we also make comparisons of the simulation cost and stability to gain a better perspective of whether new FSD models and the compressible description are favorable.

NOMENCLATURE

a	speed of sound
c	reaction progress variable
C_P	model constant for probability in Tangermann model
C_R	model constant for Tangermann model including C_P
C_s	Smagorinsky constant
C_v	model constant for k_{sgs}
D_f	fractal dimension
f	model constant in Chakraborty's model
h	step height
k_{sgs}	subgrid scale kinetic energy
L	characteristic length of domain
L_i	amplitude of characteristic wave variations for i^{th} component
M	maximum Mach number in the flow
p	pressure
p_0	initial pressure
p_∞	pressure at infinity
$P_{c,\Delta}$	probability density function
S_L	laminar flame speed
S_T	turbulent flame speed
t	time
T	temperature
T_u	unburnt temperature
T_b	burnt temperature
T_f	Period corresponding to 50Hz
$\mathbf{u}$	flow velocity vector

*Address all correspondence to this author.

u	axial velocity
u'	axial velocity fluctuation
u'_Δ	subgrid scale velocity
w	transverse velocity
w'	transverse velocity fluctuation
δ_L	laminar flame thickness
Δ	filter width
$\bar{\eta}$	effective Kolmogorov scale
η_i	inner cut off scale
Γ	efficiency function
ρ	density
ρ_0	unburnt density
σ	outflow boundary coefficient
Σ	flame surface density
Σ_{gen}	generalised flame surface density
Θ	model constant in Chakraborty's model
ν	kinematic viscosity
ν_t	turbulent kinematic viscosity
Ξ	wrinkling factor

1 Introduction

With the enforcement of stricter emission regulations, lean premixed combustion is becoming a common mode of combustion for gas turbines due to its advantage of low NO_x emissions. However, under these conditions, combustion instabilities are prone to occur and according to Rayleigh [4], the generated oscillations will be self-sustaining if a proper phase relationship exists between the heat release rate and the pressure oscillations. The oscillations will lead to enhanced vibration and reduced life-time of the combustor. In the worst case, if the disturbance frequencies are close to the resonant frequency of the system, complete system failure may result. Other than examining turbulent-chemical interactions, it is hence important to analyse flame-acoustic interactions and simulate these effects. A promising tool for predicting unsteady behaviour in turbulent reacting flows is Large Eddy Simulation (LES), which is a numerical method for resolving the large scale motions while modelling the small scales. Intermittency of the flow is inherently taken into account from the resolved scales in LES, enabling turbulence characteristics in instantaneous fresh and burnt gas zones to be clearly identified. Its advantage over the classical and commonly used Reynolds Averaged Navier Stokes (RANS) approach has been outlined in review papers by Janicka and Sadiki [5], and Pitsch [6].

Challenges do, however, arise in the application of LES to premixed combustion. As combustion mainly occurs at the small scales and the flame brush is not normally resolved, models are required to describe the reaction rate. Several approaches have been attempted, including, for example, the flame front tracking technique (G-equation [7, 8]) and the use of an artificial thickened flame (ATF [9, 10]). Both techniques encounter numerical difficulties in that the first method requires a definition of an (unphysical) signed distance function G, and the second method needs proper modelling of the efficiency function which accounts for the change in turbulence-chemistry interaction due to flame thickening. If these are properly modelled, key benefits include neglecting the modelling of the chemical source for the G-equation, and describing the proper reaction of species for the ATF approach.

The other challenge of applying LES occurs in describing the combustion instabilities. Though instabilities are normally explicitly computed, proper boundary conditions are required to account for the reflection and transmission of acoustic waves. The inflow/outflow boundary conditions have been outlined by Poinsot and Lele [1] in the context of Direct Numerical Simulation (DNS) and thereafter are numerically implemented by Schönfeld and Poinsot [11], Polifke et al. [12] and Guézennec and Poinsot [13] for LES.

This work focuses on the method of using algebraic sub-grid flame surface density (FSD) models for closure of the reaction rate. Previous work has applied these models in the simulation of reactive flow through the well-documented ORACLES rig using an in-house code, 'PsiPhi', which has been used in simulations carried out by Mike et al. [14] and Olbricht et al. [15]. This work attempts to extend the previous study [2] by exploring three recently developed FSD models for the incompressible case as well as examining the effect of adding compressibility to the existing version of the code. This involves the implementation of suitable boundary conditions, in particular, exploring the effect of increasing wave reflection at the outflow boundary. Results from both incompressible and compressible versions of 'PsiPhi' are compared for a single FSD model and conclusions are drawn on the compressible code's performance and feasibility.

2 Modelling of flow using LES

Large Eddy Simulation involves explicitly computing the large scales while modelling those that are smaller than a defined filter width. The LES code solves governing equations of mass, momentum and progress variable, of which the latter is needed to account for chemically reactive flows. More specifically, solving the progress variable transport equation allows one to determine the local temperatures and chemical densities. Within these LES filtered equations are terms that require modelling such as the subgrid stresses in the momentum equation and the reaction rate. The following Section is divided into three subsections describing the two aforementioned modelling terms and the boundary conditions that were used to account for compressibility.

2.1 Closure of subgrid stresses

In the LES filtered momentum equation, the subgrid stress $(\widetilde{u_i u_j} - \tilde{u}_i \tilde{u}_j)$ is closed using the Boussinesq approximation, and the resulting turbulent viscosity ν_t is approximated using the Smagorinsky model [16] as given by:

$$\nu_t = (C_s \Delta)^2 \left| \frac{1}{2} \left(\frac{\partial \tilde{u}_j}{\partial x_i} + \frac{\partial \tilde{u}_i}{\partial x_j} \right) \right| \tag{1}$$

where u and Δ are the convective velocity and filter width respectively. The model constant C_s is initially assumed to take the value of 0.173 as suggested by Lilly [17] but previous work [2] has shown that using a 2×0.173 value resulted in a more realistic flame brush, hence the same value will be used here.

2.2 Closure of reaction rate

In premixed combustion, the progress variable c is an indicator of flame position, distinguishing areas of fresh and burnt gases with values of 0 and 1 respectively. Under Lewis number of unity and low Mach number conditions, the progress variable can be expressed as a function of temperatures: $c = (T - T_u)/(T_b - T_u)$ where subscripts u and b denote unburnt and burnt gases. In the LES context, the quantity is transported by the following equation:

$$\frac{\partial \bar{\rho} \tilde{c}}{\partial t} + \nabla \cdot (\bar{\rho} \tilde{\mathbf{u}} \tilde{c}) + \nabla \cdot [\bar{\rho} (\widetilde{\mathbf{u}c} - \tilde{\mathbf{u}} \tilde{c})] = \overline{\nabla \cdot (\rho D \nabla c)} + \bar{\dot{w}} \tag{2}$$

where ρ is the density, $\mathbf{u}$ is the flow velocity vector, D is the progress variable diffusivity, and $\dot{w}$ is the chemical reaction rate. Two terms in Eq.(2) require modelling and these are the subgrid scalar (SGS) flux $(\widetilde{\mathbf{u}c} - \tilde{\mathbf{u}} \tilde{c})$ and $\bar{\dot{w}}$. The former term is often expressed using the simple gradient assumption and this term bears less significance in LES than in RANS [2, 18]. To provide closure for $\bar{\dot{w}}$, the molecular diffusion and reaction rate can be expressed together in terms of the generalised flame surface density Σ_{gen} [19]:

$$\overline{\nabla \cdot (\rho D \nabla c)} + \bar{\dot{w}} = \overline{(\rho S_d)}_s \Sigma_{gen} \approx \rho_0 S_L \Sigma_{gen} \tag{3}$$

From Eq. (3), the surface averaged quantity of ρS_d is approximated by the product of unburnt density ρ_0 and laminar flame speed S_L. This approximation is based on the assumption that curvature effects are weak i.e. the operating conditions point to the corrugated/wrinkled flamelet regime. Boger et al. [19] further express Σ_{gen} as a function of the wrinkling factor Ξ:

$$\Sigma_{gen} = \Xi |\nabla \bar{c}| \qquad \textit{where} \qquad \Xi = \frac{\overline{|\nabla c|}}{|\nabla \bar{c}|} \tag{4}$$

An alternative definition for Ξ is the ratio of turbulent to laminar flame speed. Several algebraic models for Ξ exist and *a-priori* and *a-posteriori* analyses have been performed by Chakraborty and Klein [20] and Ma et al. [2] respectively. The following paragraphs describe four models that will be tested in this work, including one that was explored in previous study and performed relatively well. This modified version of the Fureby model [21], is used for base comparison in the present work. Of the remaining three models, one of them proposed by Chakraborty and Klein [20] follow the formulation as given by Eq.(3), while the other two models from Tangermann et al. [23] and Muppala et al. [22] model the molecular diffusion term separately. The reason for this is that the latter two models are extended for use in LES from a RANS standpoint.

The relatively well performing model that is used for base comparison in this work is one that uses the fractal approach for modelling Ξ. A modified version of the original wrinkling factor model by Fureby [21] is given by:

$$\Xi = \left(1 + \Gamma \left(\frac{u'_\Delta}{S_L} \right) \right)^{D_f - 2} \tag{5}$$

where Γ, u'_Δ, and D_f are the efficiency function, subgrid-scale velocity fluctuation and fractal dimension respectively. The efficiency function accounts for the limited ability of small vortices to corrugate the flame front and is approximated by Angelberger et. al [24] as:

$$\Gamma = 0.75 \exp \left[-\frac{1.2}{(u'_\Delta / S_L)^{0.3}} \right] \left(\frac{\Delta}{\delta_L} \right)^{2/3} \tag{6}$$

while u'_Δ is modelled using the relationship from Deardorff [25]:

$$u'_\Delta = \sqrt{\frac{2}{3} k_{sgs}} \quad ; \quad k_{sgs} = \frac{1}{(C_\nu \Delta)^2} \nu_t^2 \tag{7}$$

where Δ and C_ν are the filter width and model constant of 0.1 respectively. The value of the fractal dimension is approximated by the empirical formulation from North and Santavicca [26]:

$$D_f = \frac{2.05}{(u'_\Delta / S_L + 1)} + \frac{2.35}{(S_L / u'_\Delta + 1)} \tag{8}$$

The modified version of Fureby's model is an extension to the original such that the laminar flame speed is recovered if $u' = 0$. Most of the algebraic models, including Fureby's model, are appropriate for the wrinkled/corrugated flamelet regime. It is shown by DNS analysis [20] that under the condition of the thin reaction zone (TRZ) regime, these models over-predict Σ_{gen}. This is largely due to the fact that the tangential diffusion component of the displacement speed is neglected and this is a dominating component in the TRZ regime. Chakraborty and Cant [27] demonstrate that this term acts as a sink for flame surface density and hence neglecting it would result in over-prediction of Σ_{gen}. In response to this, Chakraborty and Klein [20] proposes an algebraic FSD model that is suitable for both corrugated flamelet (CF) and TRZ regimes, which is given as follows:

$$\Sigma_{gen} = |\nabla \bar{c}| \cdot \left[\exp\left(-\frac{\Theta\Delta}{\eta_i} \right) \right] + |\nabla \bar{c}| \left(1 - f \exp\left(-\frac{\Theta\Delta}{\eta_i} \right) \right) \times \left(\frac{\Delta}{\eta_i} \right)^{D_f - 2} \tag{9}$$

where Θ and f are model constants that take the values of 2.5 and 0.26 respectively. The model is suited for both premixed regimes because the inner cutoff scale η_i and D_f are determined based on empirical parametrization of DNS data [20]. While D_f defined here provides similar values to that from North and Santavicca [26], the inner cutoff scale is defined as a function of Karlovitz number Ka instead of the inverse surface curvature of the flame in Fureby's model. In this way, the transition of inner cutoff scale with respect to Ka is taken into account. Another benefit from Eq.(9) is the ability to revert Σ_{gen} to $|\nabla c|$ (recovering a wrinkling factor of 1) in the limit of zero filter size.

A model that does not follow the exact closure as in Eq.(3) is proposed by Muppala et al. [22]. The difference lies in the fact that the reaction source is modelled on its own i.e. $\bar{\dot{w}} = \rho_0 S_L \Sigma_{gen}$, where Σ_{gen} can be expressed by Eq.(4). This model was originally developed for RANS and later extended for LES [28]. Their simulated results have shown good correspondence with experimental data. The model is based on three parameters which are the pressure ratio p/p_0, u'/S_L, and turbulent Reynolds number Re_t. Measured flame angles of 101 different Bunsen-type flames for fuel mixtures of methane/air, ethylene/air and propane/air were used for comparison of simulated results. Best fit lines of S_T/S_L and u'/S_L were then determined for the three mixtures leading to three flame wrinkling equations. These equations differ from each other by a certain prefactor value, and as a method of combining the three equations to one, a link between the prefactor and Lewis number was found. The LES wrinkling factor equation reads:

$$\Xi = 1 + \frac{0.46}{Le} Re_t^{0.25} \left(\frac{u'_\Delta}{S_L} \right)^{0.3} \left(\frac{p}{p_0} \right)^{0.2} \tag{10}$$

where u'_Δ is determined from Eq.(7), p_0 is assumed to be atmospheric pressure, p is based on equation of chemical state, and Re_t is evaluated from u'_Δ, filter width and laminar kinematic viscosity.

A more recent model is proposed by Tangermann et al. [23] who extend the RANS combustion model devised by Lindstedt and Vaos [29] for LES. Similar to the model by Muppala et. al [22], the reaction source is modelled on its own, but the generalised flame surface density Σ_{gen} is directly determined by the fractal approach without evaluating Ξ. The authors also introduce a probability density function $P_{c,\Delta}$ which accounts for the possibility that the flame is absent within one filter width. This is given by:

$$P_{c,\Delta}(\tilde{c}) = C_P \cdot \tilde{c}(1-\tilde{c})|\nabla \tilde{c}| \cdot \Delta \tag{11}$$

where C_P is a probability coefficient. Similar to previous models, the outer cutoff scale is set to Δ but the inner cutoff scale is approximated as the effective Kolmogorov scale $\bar{\eta}$:

$$\bar{\eta} = \left(1 + \frac{\nu_t}{\nu} \right)^{-\frac{1}{2}} C_s \cdot \Delta \tag{12}$$

This ensures that for low Reynolds numbers, i.e. $\nu_t \to 0$, the source term is evaluated with a turbulent flame speed equal to the laminar flame speed since $(\Delta/\bar{\eta})$ tends to unity in the following equation:

$$\bar{\dot{w}} = C_R \rho_0 S_L \left(\frac{\Delta}{\bar{\eta}} \right)^{\frac{1}{3}} \tilde{c}(1-\tilde{c})|\nabla \tilde{c}| \tag{13}$$

where C_R is a model constant that includes C_P in Eq.(11).

2.3 Boundary conditions for compressibility effects

Though the flow through the ORACLES rig has a Mach number much lower than 0.3, compressible simulations using LES are still useful in explaining combustion oscillations that are prone to occur in premixed flames. As perturbation features are normally computed in LES, flame visualisations may help to point out the cause of unsteady reaction rates, which sustain the oscillations that are generated from the acoustic wave travelling in the combustion chamber. For example, in the ORACLES rig, periodic vortex shedding behind the backward facing steps (shown in Fig. 1) and splitter plate (for stratified flow) causes fluctuations in flame surface area leading to unsteady heat release rates. Pockets of unburnt gases appear to burn at later times downstream, affecting the acoustics of the whole system. Incompressible LES performed by Duwig and Fureby [3] emulated this instability by introducing pulsations of the bulk velocity at the inlet. In contrast, compressible simulations avoid the need of implementing artificial pulsating behaviour, giving a more realistic description of the flame.

For the reasons mentioned above, it will be useful to perform compressible simulations that involve combustion instabilities. This would require accurate control of wave reflections from computational boundaries. The method implemented in this work follows that of Poinsot and Lele [1] and was derived for Direct Numerical Simulations of turbulent reacting flows. The method is known as the Navier Stokes Characteristic Boundary Conditions (NSCBC). The process involves recasting the equations of mass, momentum and scalar transport using characteristic analysis [30] for the boundaries and thereafter requiring one to solve expressions for amplitude variations of characteristic waves L_i. Amplitude variations corresponding to waves leaving the domain at the boundaries can be evaluated by applying one-sided interpolation of interior values, while those that correspond to incoming waves require the use of Local One-Dimensional Inviscid (LODI) relations. These expressions are viewed as compatibility relations and help express unknown values of L_i's as a function of known outgoing wave quantities. After solving for L_i, the transported variables are time advanced at the boundaries using the modified governing equations. Note that the derivatives parallel to the boundaries and local viscous terms have been ignored in this work. For the ORACLES case, a subsonic inflow with fixed velocities and temperature is selected, while the outflow is set to partially reflecting. Details for these expressions of L_i (which are functions of pressure and velocity) are reviewed by Poinsot [18], and the partially reflecting characteristic of the outflow boundary is achieved by setting a coefficient σ between 0.1 to π in Eq.(14) for the incoming wave L_1.

$$L_1 = \frac{\sigma(1-M^2)a}{L}(p - p_\infty) \tag{14}$$

The variables M, L, and a in Eq.(14) denote the maximum Mach number of the flow, the characteristic length of the domain and local speed of sound respectively. The reflected wave serves to bring the mean pressure back to a value close to a pressure p_∞ (set to 1 bar in this case). Using a higher value of σ leads to larger reflection levels, while too low a value will lead to pressure drifts. The above limits for σ were proposed by Selle et al. [31] to avoid both these situations. Rudy and Strikwerda [32] have found that the optimum value of σ is around 0.27. In this work, σ values of 0.27, 1.0 and 3.0 are tested.

3 Experimental setup and numerical modelling

The details of the experimental setup and velocity measurements were reported in the paper by Nguyen [33]. Previous LES simulations have been performed by Duwig and Fureby [3] and Fureby [21] on the plane symmetric dump combustor. The rig consists of four sections with a total length of approximately 6m. The sections include: upper and lower mixing chambers of

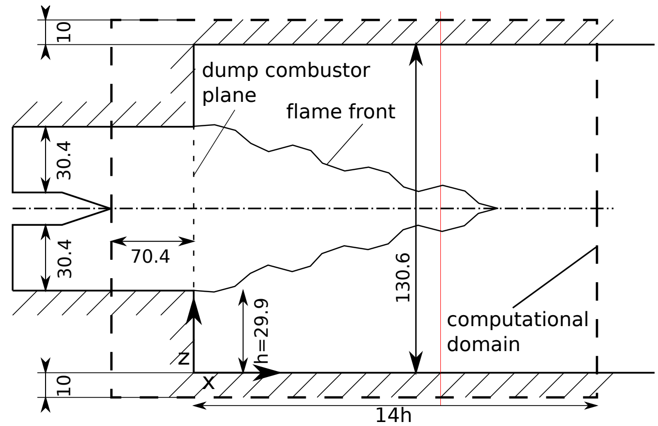

FIGURE 1. SKETCH OF THE ORACLES RIG'S COMBUSTION CHAMBER AS EXTRACTED FROM MA ET AL. [2]. INTERIOR WIDTH IN THE Y DIRECTION IS 150.4MM.

propane air, a 3m long rectangular channel divided by a splitter plate into upper and lower channels, a rectangular combustor and an exhaust. Mean and fluctuating velocities in the stream-wise and transverse directions at numerous points inside the combustor were measured using Laser Doppler Velocimetry (LDV). Figure 1 shows the area of the computational domain with the illustrated dimensions. In the present work, both feeding channels carry the same mixture of propane-air (equivalence ratio Φ=0.75) with a bulk velocity of 11m/s. The unburnt and burnt gas temperatures are 276K and 1980K respectively and the flame speed is 0.27m/s.

Large Eddy Simulation was performed with the in-house code 'PsiPhi' [14, 15], and numerically, it is a 3-D CFD code based on Darmstadt's 'flowsi' code [34–36]. Its description is briefly given in previous work [2] along with the implemented case-dependent features such as the tailored inflow and outflow conditions. The code discretises the governing equations using a finite volume approach and the convective flux of the progress variable is determined using a TVD scheme (CHARM limiter), while a second-order accurate central differencing scheme (CDS) is used for the advection term of the transport equation for momentum. At the inflow of the computational domain, the velocity profile is defined as two streams starting at the tip of the splitter plate, and the profile of each stream is described by a sixth order polynomial as given by the experiment. Turbulence is artificially generated by a method initially proposed by Klein et al. [37] and further extended by Kempf [38]. On top of this, sinusoidal pulsations of known frequency are added to account for the combustion instability. Setting the correct fluctuations for w', the amplitude has been selected to match the experimental u' values at the dump combustor plane. At the outlet, von Neumann conditions have been set for the transported quantities of mass, momentum and progress variable. As a cell size of 2mm was found to be sufficient to describe the flow features from a resolution study [2], the same resolution is selected here.

To achieve compressibility in the existing code, the net positive pressure onto each face of the computational cell was translated to net momentum flux into the cell. The pressure variable is now a physical pressure derived from an isentropic relation between pressure and densities, rather than a numerical pressure quantity that was used in the predictor-corrector algorithm [39] for incompressible flow. No energy equation is solved since the local temperatures can be derived from the equation of chemical state arising from combustion, and for these low velocities, they hardly vary with pressure. With low velocities, the kinetic energy contribution is negligible in comparison to the enthalpy terms in the energy equation (low-Mach assumption). Solving the progress variable scalar equation is thus deemed sufficient to account for enthalpy. These temperatures are then used to evaluate the local speed of sound for each cell in the domain. The governing equations are time advanced by the same low storage third-order Runge Kutta scheme as in the incompressible case, but time step width is restricted by a CFL criterion [40] that is dependent on the speed of sound rather than the convective flow speed. Time step width is thus greatly reduced and though this implies that more time steps are required to achieve statistical convergence, the longer computational time is partially compensated for by the fact that the run is more stable, iterations arising from the predictor-corrector algorithm are no longer needed, and the CFL number can be increased (in this case to 0.6). These advantages would be more apparent with higher velocity flows. The main challenge of applying compressibility to the code is the proper treatment of boundary conditions. The basic theory has been discussed briefly in Section 2.3 and in evaluating the gradients for outgoing L_i's, a first-order one sided approximation is used. Derivates parallel to the boundaries and local viscous terms are omitted when time advancing the solutions to the governing equations at the boundary. Similar to the incompressible case, sinusoidal pulsations of 50Hz are added at the inflow but the amplitude was decreased from 0.27 to 0.13 to match the velocity fluctuations at the inlet. Theoretically, these pulsations would not be implemented if the whole ORACLES rig was simulated, since the 50Hz frequency is linked to the inlet section that is 3m in length. However, performing a simulation of this scale would be cost ineffective. As the current domain is too short to recover such a low frequency, the pulsations have been added to at least match the inflow velocity fluctuations.

4 Results and discussion

The non-reactive flow through this combustor was previously simulated and presented in the paper by Ma et. al [2]. The simulated velocity results showed that the incompressible LES can deliver reasonable accuracy with a resolution of 2mm, and unlike the reactive case, the flow was asymmetric. In this Section, only the reactive case is presented and the results generated by the three FSD models are first compared with the modified version of the Fureby model for the incompressible case. Following this, a comparison of the results between the compressible and incompressible version of the code is made.

4.1 Model comparison for incompressible case

Figure 2 shows axial and transverse velocities predicted by the FSD models along with the experimental measurements. The velocity data depict a flow that is symmetric with greater acceleration near the walls of the combustor due to burnt gas expansion (about a six-fold increase in velocity near the walls compared to the non-reactive case past x = 4h in Fig. 4 of the paper by Ma et. al [2]). Combustion instability plays a role as evidenced by the elevated axial velocity fluctuations at the combustor plane ($u' \approx 2m/s$ and $w' \approx 0.6m/s$ at x = 0h) compared to those in the transverse direction. Instantaneous flame visualisations [2, 3] also support this claim and the instability is emulated by introducing pulsations at the inlet with a known frequency of 50Hz. The newly tested models present similar predictions in flow behaviour and generally match those of experimental results with less satisfactory agreement in u' at locations $x = 1h, 2h$, and $4h$ near the walls. The discrepancies suggest that the recirculation zones behind the backward facing steps are shifted slightly downstream compared to those found in the experiment. Of the three new models tested, more apparent differences occur for the Muppala model [22]. Though a closer match can be seen in mean axial velocities at downstream locations, greater over-predictions appear in mean velocities for the transverse direction. The higher chemical source leads to the lower w' near the walls since kinematic viscosity is increased. A similar effect on w' values can be seen for the Tangermann model [23]($C_R = 0.8$) but with reduced mean velocities of u and w in relation to that of the Muppala model. The model from Chakraborty and Klein [20] outputs results that resemble those of the modified Fureby model, with minor improvements in both directions. This outcome may arise from the fact that both models use the fractal approach and a more accurate estimation of η_i is applied in the Chakraborty model. Overall, the Chakraborty model seems to give the best agreement to experimental results and this is consistent with the *a-priori* DNS work by Chakraborty and Klein [20], where the model is shown to predict FSD with slightly greater accuracy than the Fureby model.

4.2 Compressibility results

Figure 5 shows a comparison of axial and transverse velocities between the compressible and incompressible codes. Apart from the location at the dump combustor plane $x = 0h$, the differences in velocity results between compressible and incompressible are obvious. The deviations clearly show that compressibility has an effect on the flow. For example, looking at mean ax-

FIGURE 3. FLAME VISUALISATIONS OF INCOMPRESSIBLE (TOP) AND COMPRESSIBLE (BOTTOM) FOR $\sigma = 3.0$ AT $t = 0.485s$. DARK AREAS REPRESENT UNBURNT GAS.

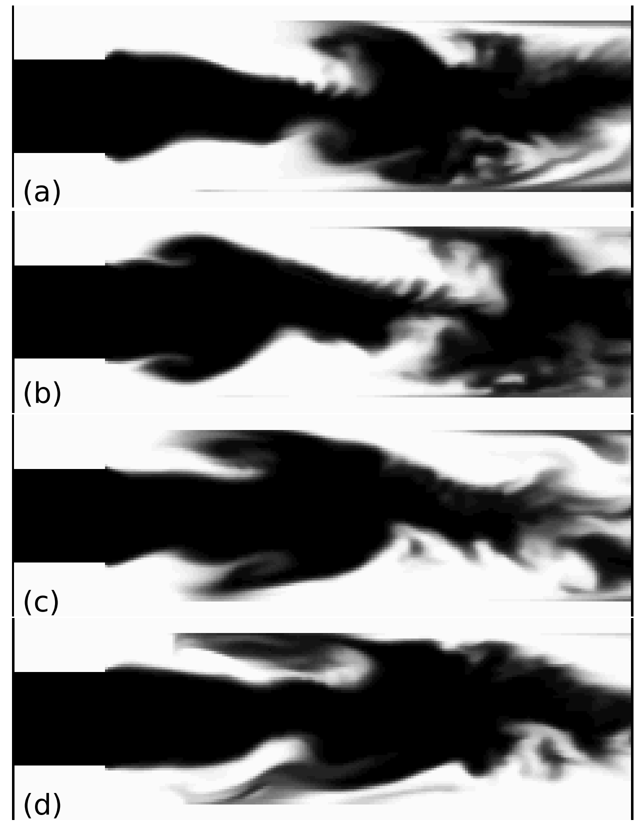

FIGURE 4. FLAME VISUALISATIONS OF COMPRESSIBLE CASE AT (a) t, (b) $t+\frac{1}{3}T_f$, (c) $t+\frac{2}{3}T_f$, (d) $t+T_f$, WHERE $t = 0.465s$ and $T_f = 0.02s$

ial velocities, large under-predictions occur at downstream locations, and instantaneous flame visualisations (Fig. 3) taken from the same flame time reveal that this is due to a larger proportion of unburnt gases travelling downstream of the domain than for the incompressible case. Trails of these gases reside near the top and bottom walls of the combustor for a longer period of time before being consumed, hence the reduced flow acceleration in these regions. A series of images for the compressible case showing a full cycle of 50Hz ($T_f = 0.02s$) starting from $t = 0.465s$ are displayed in Fig. 4. Pockets of unburnt gases travelling downstream of the domain are clearly shown.

Interestingly, the axial velocity fluctuations maintain magnitudes close to the experimental and incompressible results throughout the domain, suggesting some similarities on the influence of the flame on turbulence. Velocities in the transverse direction however show more promising results. In the previous work [2], we have stated that there are discrepancies between the simulated values of w' and experimental data due to lack of modelling combustion instability effects. Though slightly overpredicting, the compressible results show a closer match of w' to experimental data (especially past $x = 2h$) and improvements are also apparent in mean transverse velocities, showing less overpredictions.

As mentioned in Section 2.3, σ is a variable parameter defining the amplitude of wave reflections incurred by the outflow boundary. To investigate its effect, three different values of σ are used and it is found that using a higher σ value accelerates the flow in the stream-wise direction. This is the result of increasing the amplitude of wave reflections causing greater wrinkling of the turbulent flame. Flame surface area is thus increased leading to a larger chemical source and higher mean velocities. The increase in σ proves to be generally beneficial though it is not enough to match the experimental values for the axial mean velocities. The maximum value of σ tested in this work lies close to the upper limit of the optimal range $0.2<\sigma<\pi$ as proposed by Selle et al. [31] in order to avoid both mean pressure drifts and large reflection coefficients which may be unrealistic. It would be interesting to explore even higher values of σ, however, one must note that adding pulsations for the compressible code makes less physical sense and as mentioned earlier, the 6m long rig would need to be simulated in order to achieve the low frequency, albeit at a substantially higher computational cost, with the added difficulty that wave propagation and turbulent boundary layers in the feeding channel would have to be resolved accurately, at an even higher computational cost.

The compressible case took around 976 CPUh to achieve statistical convergence and this is more than 5 times more computationally expensive than for the incompressible case. However, this is a cost that can be well justified if thermo-acoustic interactions can be recovered. Furthermore, the ORACLES case is somewhat unusual for its low velocities, where an increase would equalise the cost of incompressible and compressible methods.

5 Conclusions

Three FSD models that were recently developed were simulated and compared with a modified version of the model by Fureby [21]. The models have shown good predictions as their velocity results follow closely to those of the modified Fureby model. The model by Chakraborty and Klein [20] showed very minor improvements over the modified Fureby model and therefore a slightly better agreement with experimental results. It was previously reported by Nguyen et al. [33] that combustion instabilities occurred in this test case due to flame-acoustic coupling, and Duwig and Fureby [3] have emulated these effects by introducing pulsations at a given frequency to their incompressible code. The same technique was applied to simulations in previous work [2], and as a way of simulating combustion instabilities more accurately, compressibility has been introduced to the existing code. This mainly involved applying a physical pressure to the momentum field as a replacement for the more costly projection method, and implementing new treatments to the computational boundaries. A subsonic inflow with fixed velocity and temperature as well as a partially reflecting outflow are implemented based on NSCBC [1]. As it would be cost-ineffective to simulate the whole rig, pulsations with a lower amplitude were also added to the inlet in an attempt to recover similar effects on the flow field from a 50Hz frequency wave. The results generated showed obvious differences with mean axial velocities under-predicting the experimental data due to the greater proportion of unburnt gases propagating downstream. Interestingly, axial fluctuations maintain a decent order of magnitude and velocities in the transverse direction show much better resemblance to experimental data. Fluctuating velocity peaks that were poorly captured for the incompressible case in the transverse direction were shown to improve with compressibility. Parametric studies were carried out to vary the amplitude of reflections at the outflow and using higher values of σ has shown improved results. As suggested by one reviewer, it would be interesting to compare the predictions for cold flow in order to further validate the merits of using FSD models and compressibility. This will preferably be explored in a more suitable test case at a later stage. Overall, both incompressible and compressible simulations give decent results.

The compressible code runs more stably than its incompressible counterpart, and with optimised code parallelisation, run times will reduce. We have seen that despite not simulating the whole rig, we were able to achieve results that were comparable to experimental data.

ACKNOWLEDGMENT

The authors acknowledge the financial support provided by the ESPRC through grant: EP/G008841/1.

REFERENCES

[1] Poinsot, T., and Lele, S., 1992. "Boundary conditions for direct simulations of compressible viscous flows". *Journal of Computational Physics,* ***101***, pp. 104–129.

[2] Ma, T., Stein, O., Dorri, L., Chakraborty, N., and Kempf, A. *A-posteriori* comparison of algebraic flame surface density models for LES. Submitted to Combustion and Flame 2010.

[3] Duwig, C., and Fureby, C., 2007. "Large eddy simulation of unsteady lean stratified premixed combustion". *Combustion and Flame,* ***151***, pp. 85–103.

[4] Rayleigh, L., 1896. *The Theory of Sound*, 2nd ed. Macmillan.

[5] Janicka, J., and Sadiki, A., 2005. "Large eddy simulation of turbulent combustion systems". *Proceedings of the Combustion Institute,* ***30***, pp. 537–547.

[6] Pitsch, H., 2006. "Large-eddy simulation of turbulent combustion". *Annual Review Fluid Mechanics,* ***38***, pp. 453–482.

[7] Düsing, M., Kempf, A., Flemming, F., Sadiki, A., and Janicka, J., 2005. "Combustion LES for premixed and diffusion flames". *Progress in Computational Fluid Dynamics, an International Journal,* ***7***, pp. 363–374.

[8] Pitsch, H., and Lageneste, D. D., 2002. "Large-eddy simulation of premixed turbulent combustion using a level-set approach". *Proceedings of the Combustion Institute,* ***29***, pp. 2001–2008.

[9] Freitag, M., 2007. "On the simulation of premixed combustion taking into account variable mixtures". PhD thesis, TU Darmstadt.

[10] Roux, S., Lartigue, G., Poinsot, T., Meier, U., and Bérat, C., 2005. "Studies of mean and unsteady flow in a swirled combustor using experiments, acoustic analysis, and large eddy simulations". *Combustion and Flame,* ***141(1-2)***, pp. 40–54.

[11] Schönfeld, T., and Poinsot, T., 1999. "Influence of boundary conditions in LES of premixed combustion instabilities". *Centre for Turbulence Research (Annual Research Briefs)*, pp. 73–84.

[12] Polifke, W., Wall, C., and Moin, P., 2006. "Partially reflecting and non-reflecting boundary conditions for simulation of compressible viscous flow". *Journal of Computational Physics,* ***213***, pp. 437–449.

[13] Guézennec, N., and Poinsot, T., 2009. "Acoustically nonreflecting and reflecting boundary conditions for vorticity injection in compressible solvers". *AIAA,* ***47***, pp. 1709–1722.

[14] Pettit, M., Coriton, B., Gomez, A., and Kempf, A., 2010. "Large-eddy simulation and experiments on non-premixed highly turbulent 'opposed jet' flows". *Proceedings of the Combustion Institute,* ***doi: 10.1016/j.proci.2010.06.140***.

[15] Olbricht, C., Janicka, J., and Kempf, A., 2010. "LES as

a prediction tool for lifted flames in a model gas turbine combustor". *ASME Turbo Expo 2010: Power for Land, Sea and Air*.
[16] Smagorinsky, J., 1963. "General circulation experiments with the primitive equations i. the basic experiment". *Monthly Weather Review, **91(3)***, pp. 99–164.
[17] Lilly, D., 1967. "The representation of small-scale turbulence in numerical simulation experiments". *Proceedings of the IBM Scientific Computing Symp. on Environmental Sciences*, pp. 195–210.
[18] Poinsot, T., and Veynante, D., 2005. *Theoretical and Numerical Combustion*, 2nd ed. R.T. Edwards, Philadelphia, PA, USA.
[19] Boger, M., Veynante, D., Boughanem, H., and Trouve, A., 1998. "Direct numerical simulation anaylsis of flame surface density concept for large eddy simulation of turbulent premixed combustion". *Twenty-Seventh Symposium (International) on Combustion/The Combustion Institute, **27***, pp. 917–925.
[20] Chakraborty, N., and Klein, M., 2008. "A priori direct numerical simulation assessment of algebraic flame surface density models for turbulent premixed flames in the context of large eddy simulation". *Physics of Fluids, **20***, p. 085108.
[21] Fureby, C., 2005. "A fractal flame-wrinkling large eddy simulation model for premixed turbulent combustion". *Proceedings of the Combustion Institute, **30***, pp. 593–601.
[22] Muppala, S., Aluri, N., Dinkelacker, F., and Leipertz, A., 2005. "Development of an algebraic reaction rate closure for the numerical calculation of turbulent premixed methane, ethylene, and propane/air flames for pressures up to 1.0 MPa". *Combustion and Flame, **140***, pp. 257–266.
[23] Tangermann, E., Keppeler, R., and Pfitzner, M., 2010. "Premixed turbulent combustion models for large eddy and rans simulations". *Proceedings of ASME Turbo Expo 2010: Power for Land, Sea and Air, **GT2010-22298***.
[24] Angelberger, C., Veynante, D., Egolfopoulos, F., and Poinsot, T., 1998. "Large eddy simulations of combustion instabilities in premixed flames". *Proceedings of the Summer Program (Center for Turbulence Research)*, pp. 61–82.
[25] Deardorff, J., 1980. "Stratocumulus-capped mixed layers derived from a three-dimensional model". *Boundary-Layer Meteorology, **18***, pp. 495–527.
[26] North, G., and Santavicca, D., 1990. "The fractal nature of turbulent premixed flames". *Combustion Science and Technology, **72***, p. 215.
[27] Chakraborty, N., and Cant, R., 2007. "A priori analysis of the curvature and propagation terms of the flame surface density transport equation for large eddy simulation". *Physics of Fluids, **19***, p. 105101.
[28] Aluri, N., Muppala, S., and Dinkelacker, F., 2008. "Large-eddy simulation of lean premixed turbulent flames of three different combustion configurations using a novel reaction closure". *Flow, Turbulence and Combustion, **80***, pp. 207–224.
[29] Linstedt, R. P., and Vaos, E. M., 1999. "Modeling of turbulent flames with second moment methods". *Combustion and Flame, **116***, pp. 461–485.
[30] Thompson, K., 1987. "Time dependent boundary conditions for hyperbolic systems". *Journal of Computational Physics, **68***, p. 1.
[31] Selle, L., Nicoud, F., and Poinsot, T., 2004. "The actual impedance of non-reflecting boundary conditions: implications for the computation of resonators". *AIAA, **42***, pp. 958–964.
[32] Rudy, D., and Strikwerda, J., 1980. "A non-reflecting outflow boundary condition for subsonic navier stokes calculations". *Journal of Computational Physics, **36***, pp. 55–70.
[33] Nguyen, P., Bruel, P., and Reichstadt, S., 2009. "An experimental database for benchmarking simulations of turbulent premixed reacting flows: Lean extinction limits and velocity field measurements in a dump combustor". *Flow Turbulence Combustion, **82***, pp. 155–183.
[34] Stein, O., Kempf, A., and Janicka, J., 2007. "LES of the sydney swirl flame series: An initial investigation of the fluid dynamics". *Combustion Science and Technology, **179***, pp. 173–189.
[35] Kempf, A., Malalasekera, W., Ranga-Dinesh, K., and Stein, O., 2008. "Large eddy simulations of swirling non-premixed flames with flamelet models: A comparison of numerical methods". *Flow Turbulence Combustion, **81***, pp. 523–561.
[36] Renfro, M., Chaturvedy, A., King, G., Laurendeau, N., Kempf, A., Dreizler, A., and Janicka, J., 2004. "Comparison of oh time-series measurements and large-eddy simulations in hydrogen jet flames". *Combustion and Flame, **139***, pp. 142–151.
[37] Klein, M., Sadiki, A., and Janicka, J., 2003. "A digital filter based generation of inflow data for spatially developing direct numerical of large eddy simulation". *J. Comput. Phys., **186***, pp. 652–665.
[38] Kempf, A., Klein, M., and Janicka, J., 2005. "Efficient generation of initial- and inflow-conditions for transient turbulent flows in arbitrary geometries". *Flow Turbulence Combustion, **74***, pp. 67–84.
[39] Kempf, A., 2003. "Large-eddy simulation of non-premixed turbulent flames". PhD thesis, TU Darmstadt, Germany.
[40] Courant, R., Friedrichs, K., and Lewy, H., 1967. "On the partial difference equations of mathematical physics". *IBM Journal*, pp. 215–234.

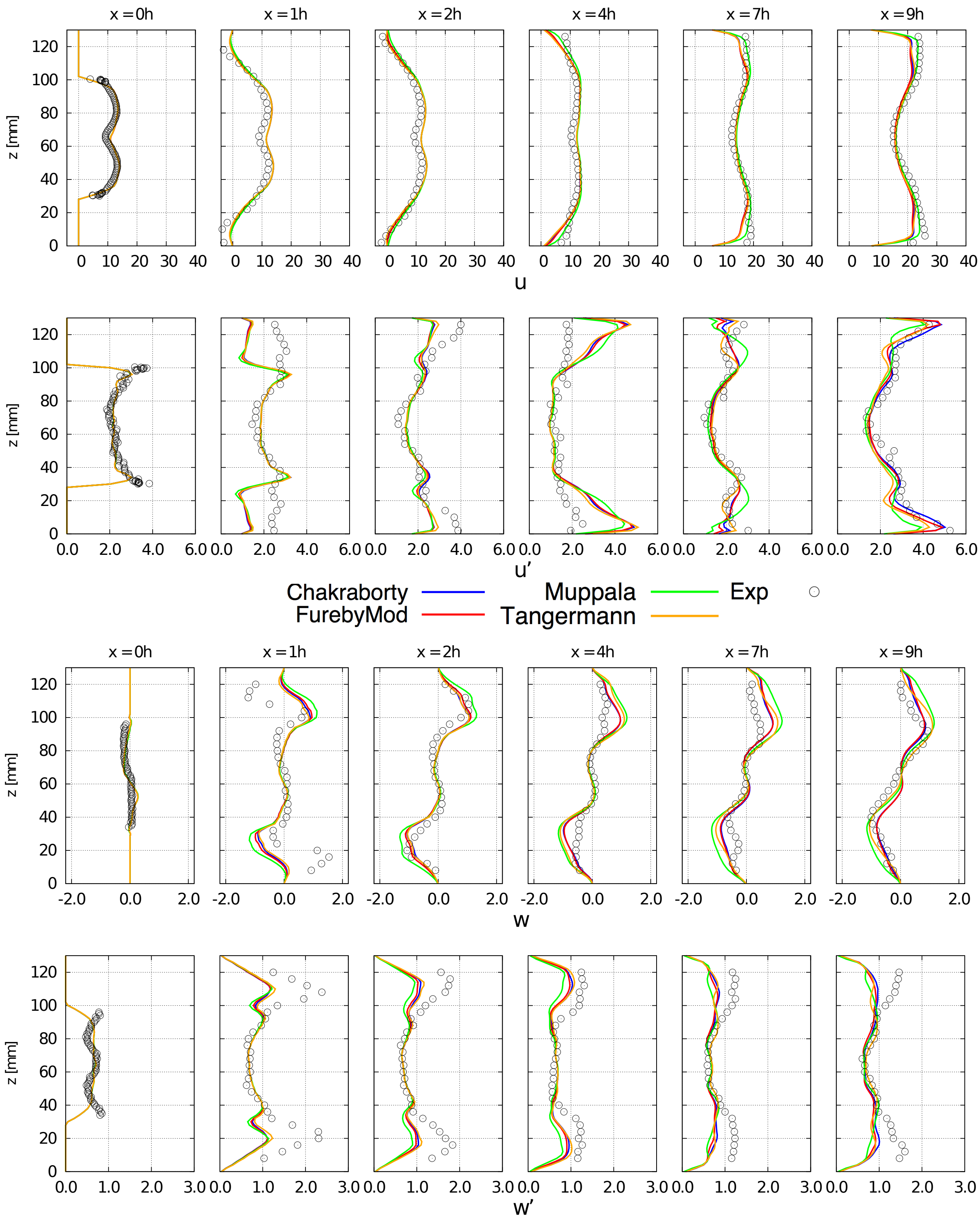

FIGURE 2. MEAN AND FLUCTUATING VELOCITIES FOR DIFFERENT FSD MODELS.

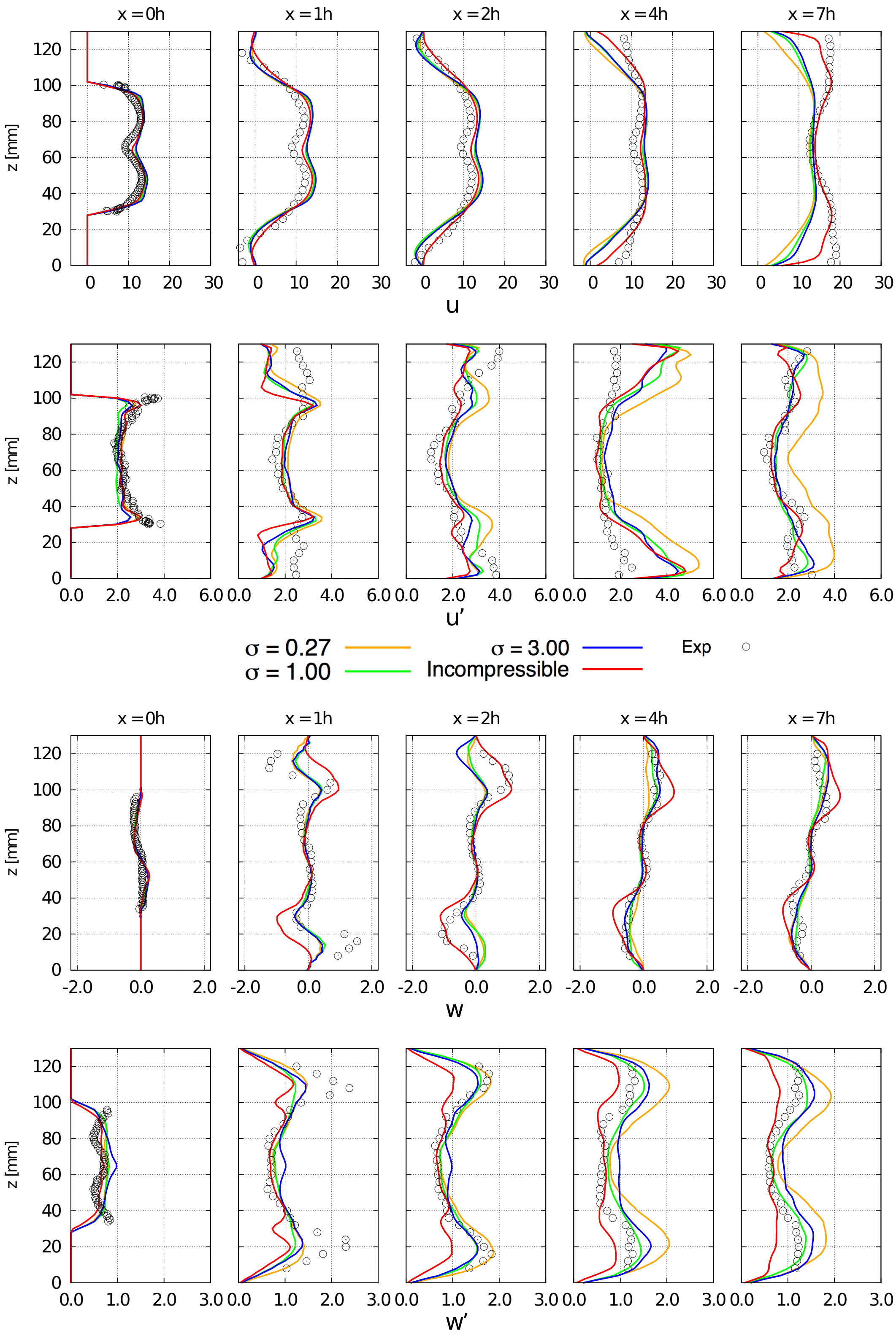

FIGURE 5. MEAN AND FLUCTUATING VELOCITIES COMPARING COMPRESSIBILITY AND INCOMPRESSIBILITY.